Arabian Journal of Geosciences (2021) 14: 664
https://doi.org/10.1007/s12517-021-06641-2

ORIGINAL PAPER

Developing new geophysical scanners for detection of near-surface buried objects

Fouzan A. Alfouzan[1] · Khaled Bakkour[2] · Bing Zhou[3] · Mazen M. Alyousif[1]

Received: 7 April 2018 / Accepted: 23 January 2021 / Published online: 4 April 2021

Abstract

A new fusion of geophysical scanners is developed for detection of the near-surface buried objects, such as iron pipes, pieces of metal, and rocks. The new fusion was built up in a cart that integrates three kinds of geophysical instruments including an EM-61 metal detector, magnetometer, and OhmMapper. For the new system, we have innovate an electric control unit and adapted all the original connection cables to efficiently and simultaneously collect the electromagnetic field, magnetic intensity, and apparent resistivity on the surface of ground. We also modified and complement DOS-based computer programs to automatically measure the three kinds of data, record the surveying positions, and transfer the data from the system to a host computer for integration of the mapping images. The new system has been tested at a synthetic field site where five different objects are previously buried. The experimental results show successes in mapping these near-surface targets and prove that the new system archives saving surveying time, obtaining comprehensive data, reducing human interventions and number of human operators. It may become a new efficient and effective tool of geophysical exploration for detection of the near-surface buried objects.

Keywords Electromagnetics · Magnetics · Resistivity · Buried targets · Near-surface detection

Introduction

Geophysical exploration techniques, such as electromagnetic prospecting (Telford et al. 1990; Zhdanov 2017), electrical resistivity measurement (Loke 2011), and gravitational and geomagnetic measurements (Keating and Sailhac 2004), are all geophysical tools for mapping the subsurface natural resources, detecting the near-surface buried targets and geological structures, exploring underground environments, monitoring geological hazards. Always recommend to run and apply several geophysical techniques to map and acquire a complete information on subsurface structures of the physical properties, due to difference in sensitivity to physical properties of rocks. Therefore, to collect the conductivity or resistivity of the media underneath, the electrical resistivity technique is always applied, and for the magnetic permeability and permittivity, to which the electromagnetic prospecting are most sensitive, while for the gravitational and geomagnetic measurements are recommended to find underground targets that have significant variations in term of density and magnetism. Of course, there are some limitations of the geophysical techniques that may cause defective or multiple images of the underground. Therefore, practical applications become important to integrate or combine of different geophysical techniques, as it may complement the information on the physical properties to each other and yield a unique geological model.

Many attempts to develop various geophysical systems have been made during the last decades between specialized companies and research institutes to explore what lies underneath, metal detector (Breiner 1999), magnetometer (Geometrics 1995; Hinze et al. 2013), and OhmMapper (Geometrics 2001). These geophysical instrumentations are considered as the non-destructive techniques for investigating and exploring the subsurface from the surface without digging, probing, or drilling. They are often used to locate and map many types of buried objects and features. However, the main problem with those systems is that integration of the

Responsible Editor: Narasimman Sundararajan

✉ Fouzan A. Alfouzan
alfouzan@kacst.edu

[1] National Centre for Oil & Gas Technology, King Abdulaziz City of Sciences & Technology (KACST), Riyadh, Saudi Arabia

[2] R&D Department, Nanotechnologies Est, Riyadh, Saudi Arabia

[3] Petroleum Geosciences, The Petroleum Institute, Abu Dhabi, United Arab Emirates

geophysical scanning surveys is a time-consuming process because different types of equipment, each of which, have to be employed in the survey that covers the same working area and independent data processing. In order to efficiently carry out these geophysical surveys, we have attempted to integrate different types of geophysics scanners and come up with single comprehensive equipment capable of delivering multiple kinds of data that is originally provided by the individual instrument (sub-systems). The integrated system includes EM-61 metal detector, magnetometer or gradiometer, and OhmMapper, which are controlled by our developed electric control unit and a Dos-commanded program so that the three kinds of data are simultaneously collected and transferred to the host computer. The new system brings benefits to field survey in four aspects: (a) saving data-acquisition time, scanning a specific piece of land one time instead of scanning it separately with each scanner; (b) obtaining comprehensive information, one system includes all sub-systems; (c) reducing human intervention, the system operates almost by itself; and (d) reducing number of operators, one single operator operates the integrated system. This paper will show the key components of the system and its field-testing experiments. The measurement results demonstrate the capability of the new system to capture different buried objects at a synthetic field site.

Three scanners

EM-61 metal detector

The EM-61 metal detector (Geonics Limited 2010) is a contactless scanner and works by sending vertical magnetic wave via one transmitter coil and measuring the voltage (mV) generated at the ends of two receiver coils (see Fig. 1). The lower coil exists in the same frame containing the transmitter coil. The second coil has its own frame located 28cm above the first coil. The coil assembly has the shape of rectangular prism having length of 100cm, width of 50cm, and height of 28cm with two detachable wheels. One of those wheels has a built-in odometer with step of 19.3 cm. This instrument records the secondary magnetic intensities (Tesla) by four channels $\left\{B_i^{(1)}, B_i^{(2)}, B_i^{(3)}, B_i^{(4)}\right\}$ at each observation position (x_i, y_i). To conduct a survey with EM-61, the operator has to begin by setting all configuration parameters on the console. Once done, he starts the survey at the original point (mark 0, line 0) and pushes the device forward (or pull it) along the lines of the surveyed site. The internal odometer will be responsible to automatically make marks along the surveyed line. The operator has to continue this way until he reached the end point at the last line.

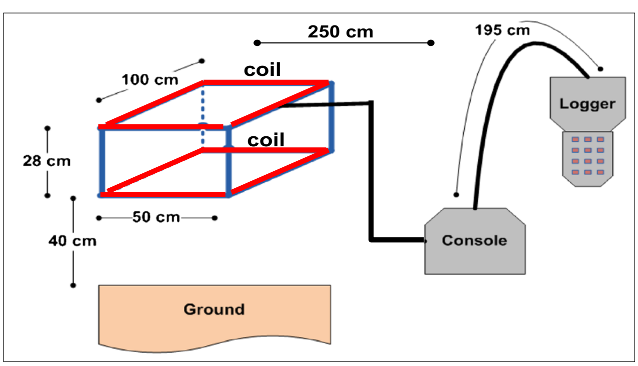

Fig. 1 A metal detector, which is showing a simple illustration for the EM61 metal detector layout, and connectivity covering the exact dimensions, and cable lengths

Magnetometer

The magnetometer scanner or gradiometer (Geometrics 1995) is also a contactless scanner that has a shape of a triangular wheeled cart with a central pole holding the two sensors vertically and concentrically (see Fig. 2). The cart is made of aluminum alloy to eliminated interference and noise. It transmits radio frequency signals, detects the reflected signals, and logs the data accordingly.

The cesium vapor magnetometer is based on alkali vapor. The device broadly consists of a photon emitter containing a cesium light emitter or lamp, an absorption chamber containing cesium vapor, a "buffer gas" through which the emitted photons pass, and a photon detector, arranged in that order. Cesium magnetometers can measures the total magnetic field B_i^{MG} up to 30,000 nT.

OhmMapper

The OhmMapper scanner is a chain of components that need to be laid down on the surface under inspection (see Fig. 3) and the operator conducts the survey by pulling the chain behind him. The chain is formed of a dummy weight to force the rest of the components to touch the surface, a receiver that is connected to the console held by the operator, and a

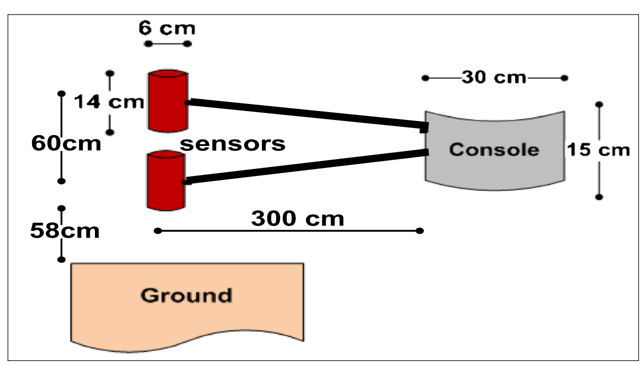

Fig. 2 A magnetometer, which is showing a simple illustration for the magnetometer layout, and connectivity covering the exact dimensions and cable lengths

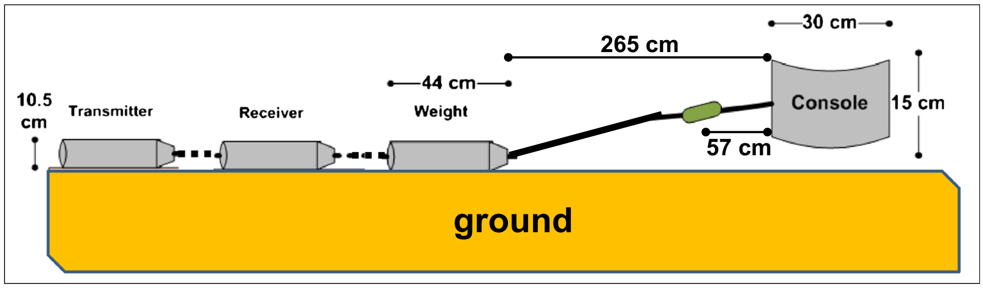

Fig. 3 An OhmMapper, which is showing a simple illustration for the OhmMapper layout, and connectivity covering the exact dimensions, cable lengths, and junction location

transmitter connected to the receiver at a predefined distance via a non-conductive rope. The transmitter and the receiver have the shape of a cylinder with two cable (dipole cable) connected to both ends. Those dipole cables play the role of the antenna that transmit the signal and receives them. Its method of operation is based on the usage of multiple electric and electronic laws including Maxwell's equations, so that the apparent resistivity $(\rho_a)_i$, reactance measurement, and impedance measurement of the soil underneath are measured at the mid-point (x_i, y_i) between the transmitter and receiver. Different spaces between transmitter and receiver reflect on different measurement depth. The wider the distance between the transmitter and the receiver, the deeper the measurement penetrates. Two measurement modes are often employed: plan-view map and pseudo-section. The former is produced when a site is surveyed by using a fixed transmitter-receiver separation on a number of adjacent lines and the latter is carried out when the same profile line is surveyed several times with different transmitter-receiver separations.

As shown above, each scanner has its own operator during the survey, and once done, the operator has to connect his scanner console to the host computer to dump the data acquired during the survey. Figure 4 is a sketch of field surveys of the three scanners. The drawing has all scanners and operators located next to each other, but in fact, every operator conducts his survey alone, independently of his colleagues.

New cluster system

The three scanners described in the previous section are referred to as sub-systems and integrated in our new system that looks like shown in Fig. 5. One single operator is needed to run the new system, as the scanners are connected to an electronic control unit and connected to the host computer by one single port.

However, from our experience of dealing with those equipment, there were some major concerns to which we had to pay attentions during integration of multi-system development. They may include three aspects: (1) all sub-systems operate in the electromagnetic spectrum so that interference becomes a major issue; (2) the sub-systems have different data interface and different transmission protocols, which require a control unit to manager data acquisition, storage, display, and transformation; (3) the sub-systems are very sensitive to the surrounding objects, e.g., the most sensitive scanner is the magnetometer. It could detect the smallest metallic item in its range in addition to items existing around it like wristwatches, belt clips, and even keys.

Electric control unit

In order to control the sub-systems, the electronic control unit (ECU) shown in Fig. 5 has been designed. Figure 6 is the

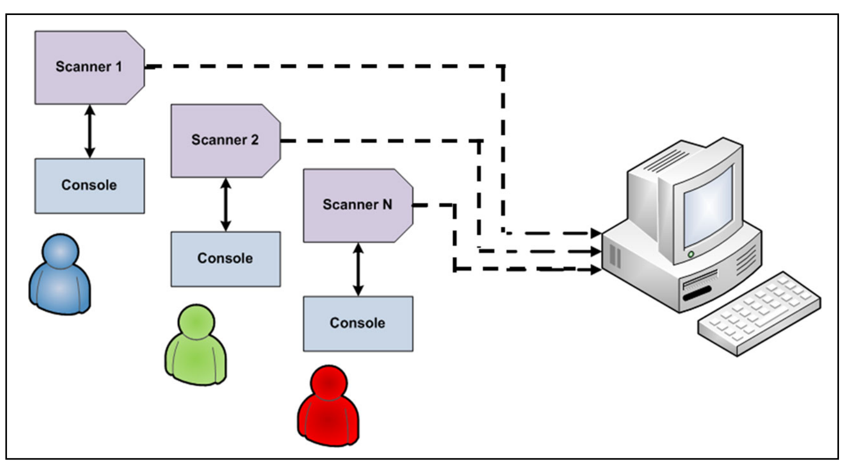

Fig. 4 Scanners' original setup, where each scanner has its own operator during the survey, and once done, the operator has to connect his scanner console to the host computer to dump the data acquired during the survey. For demonstration purposes, the drawings have all scanners and operators located next to each other, but in fact, every operator conducts his survey alone, independently of his colleagues

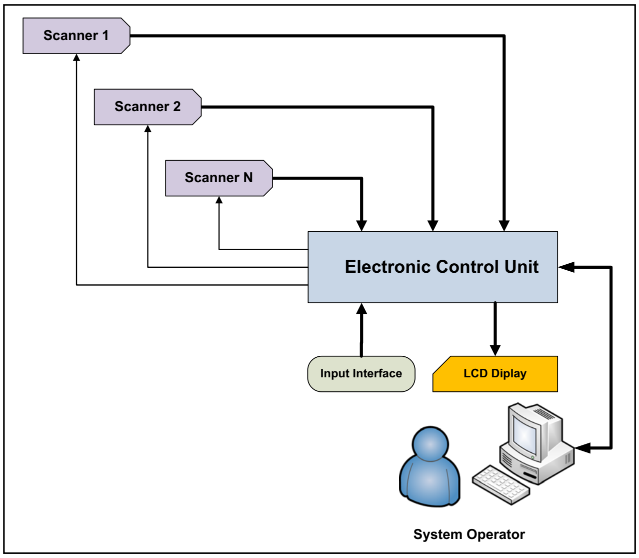

Fig. 5 The expected system, where all the scanners are connected to the electronic control unit. It requires only one single operator and one single port to be connected to the host computer

block diagrams for the ECU, which is to be integrated within the new system, is connected to the sub-system all the time, and has a single port to connect it to the host computer where all surveying data are dumped. The heart of the ECU is the central processing unit (CPU), which is composed of the following modules:

a. Data acquisition registers that hold the values read from the user input interface.
b. Data register is where all variables and constants are stored for later fetching and processing by the arithmetic and logic unit (ALU).
c. Multiplexers are used by the CPU for selecting which input to be fed into the ALU.
d. ALU is the module that processes all calculations and logical operations
e. Working register is the register that holds intermediate operation results performed by the ALU before being reprocessed again.

In addition to those main modules, the CPU can communicate with other type of devices by having theses following interface modules.

a. The power interface plays the role of a simple buffer that increases the power of the signals generated by the ALU before being interfaced to other electronic components.
b. The string manipulation module converts the CPU signal into characters to be interfaced later on to an LCD display.
c. The LED array interface is another kind of buffers that amplifies a group of interfacing lines instead of a single line.

Fig. 6 Represents the block diagram for the electronic control unit. The heart of the ECU is the central processing unit, which is composed of the many modules

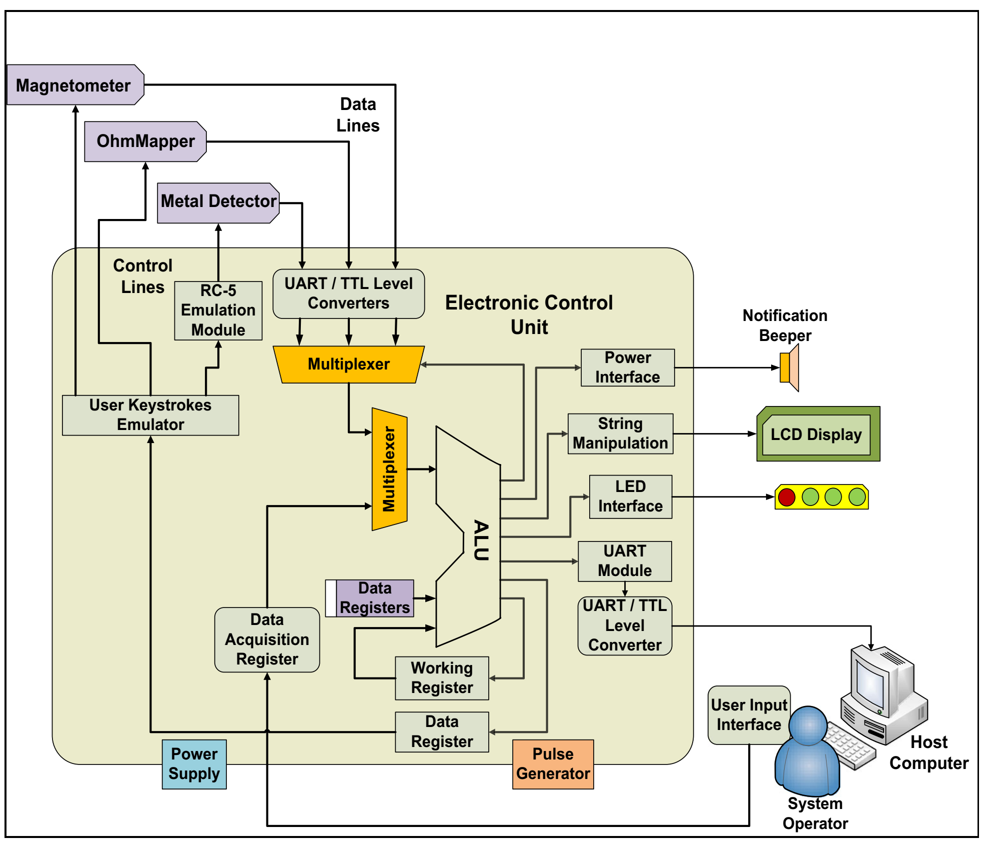

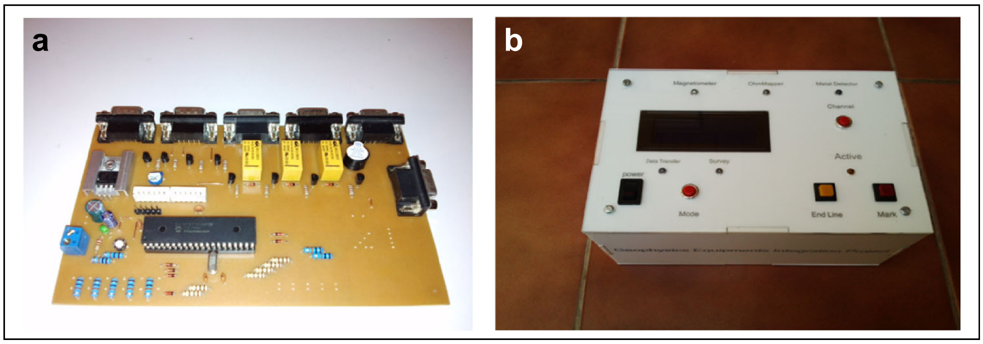

Fig. 7 Showing the electronic control unit after implementation (a) electronic control unit after soldering the components (b) electronic control unit prototype

d. The UART module (universal asynchronous receiver/transmitter) is the interface responsible for transmitting and receiving signals serially from and to the CPU. This module allows the communication with serial devices like computer serial ports.
e. The UART/TTL level converters are the serial protocol-level converters used to convert TTL signal to RS232 signals and vice versa.
f. The user keystrokes emulator is the interface responsible of controlling the external sub-systems during surveys.
g. The RC-5 emulation module is a special serial data transmission interface that uses Manchester encoding developed for sending RC-5 bit streams to emulate keystrokes on the metal detector handheld. This module has corresponding software developed and installed on the handheld.

The last two blocks in the CPU are:

a. Power supply module that provides regulated +5V DC.
b. Pulse generator (also called clock) which is a necessary input signal to the CPU to operate.

In addition to CPU, the ECU includes the following peripherals.

a. A notification beeper that generates audible sounds.
b. A character LCD display that will instruct the driver which direction he has to take and which parking lot is closer to him.
c. A set of LED used to indicate various functions when the system is in duty.
d. A serial connector to connect the ECU to a computer where the survey data duping software(s) are hosted.
e. Serial connectors to connect the ECU to the external sub-systems.
f. User interface, which is a set of buttons and switches mounted on a handheld for the system operator to control the sub-systems during surveys.

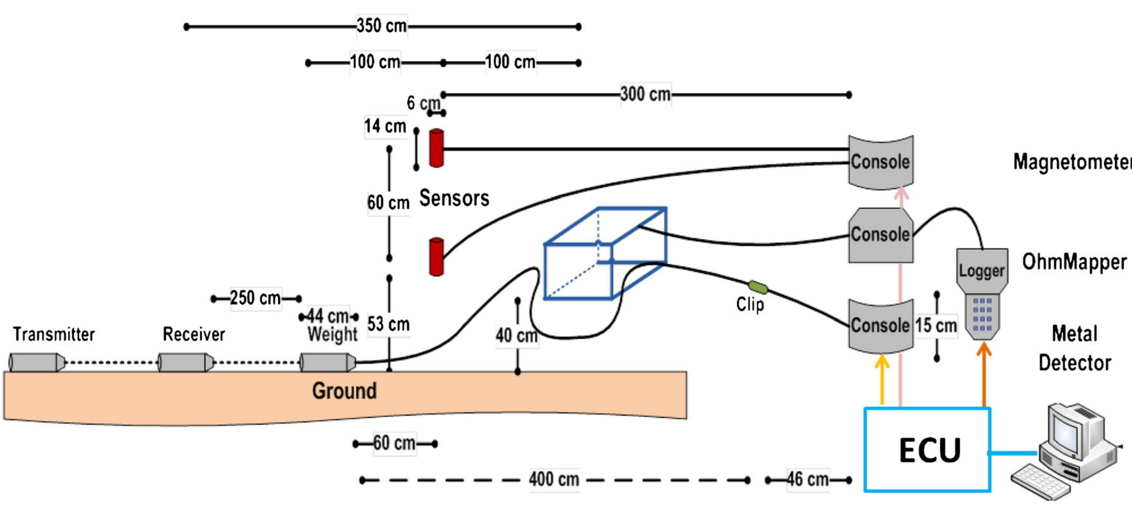

Fig. 8 Showing the sensor sequence, the loop coil assembly of the metal detector comes first, the cesium vapor sensors of the magnetometer are placed at 100 cm away from the center of the coils, and the dummy weight of the OhmMapper shall be place 60 cm away from the cesium vapor sensors. The 180-cm dipole cable connecting the tow cable of the OhmMapper to the optical wand inside the dummy weight was replaced by the 400-cm cable to facilitate the routing of the cable around the coil assembly without affecting the distance between the cesium vapor sensor and the dummy weight

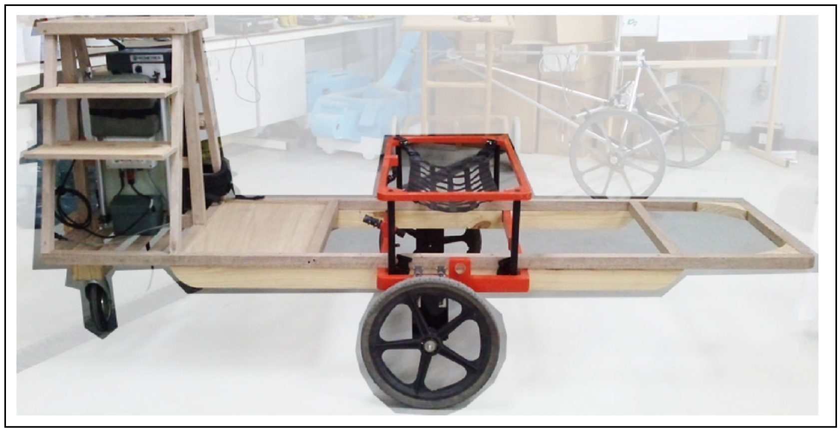

Fig. 9 Initial cart, all constrains and recommendations were taken into considerations, the implemented design was quite long. The total length of the cart was 275 cm as shown

As noticed in the block diagram, there are two types of connections between the sub-systems and the ECU. One is data lines and other is control lines. The data lines are two-way communication lines used when transferring surveying data into the host computer. The control lines are one-way communication lines used when conduction surveys to eliminate human interaction with the sub-systems. Figure 7 shows the soldering components and prototype of the ECU, which replace the human operators for the different scanners and control the scanners consoles automatically during survey. The system operator shall be dealing with all the scanners as if it is one scanner, and the ECU shall take care of the rest. At every survey, the operator needs to manually configure all the sub-systems, and get them ready to start the scanning survey where the ECU takes control. After finishing a survey, the data transmission from the system to the host computer is also controlled by the ECU. At this stage, the operator connects data-port of the ECU with host computer and then selects which sub-system to transfer the data from. The ECU performs selection of the proper data transfer protocol, transmission speed, and fetching data from the sub-systems to the computer. In addition, the ECU has an audio-visual reporting system to inform the operator about the task being processed at any given time. A grip remote control (Gripmote) has been also designed. The system operator will hold a wired handheld remote control during survey mode. It has mainly two buttons "Mark" and "End Line." In addition, it has an internal beeper and a LED (see Fig. 7b). When in survey mode, the LED will be ON to indicate that the Gripmote is active, and keystrokes are sent to the ECU. In data transfer mode, the Gripmote will be inactive, and the LED will be off. The internal beeper is used to audibly inform the user about actions being taken by the system during surveys.

Cart design

The shape of cart holding all the sub-systems is subject to some constrains which are shapes and dimensions of the sensors (transceivers), measurement cables lengths, and interference between sensors. The best layout for the sensors is to have the metal detector loop coils placed first and the rest should be place behind as shown Fig. 8. The loop coil

Fig. 10 The mini cart picture in the field was taken during a real test conducted to make sure that all the system were working properly without interference among each other

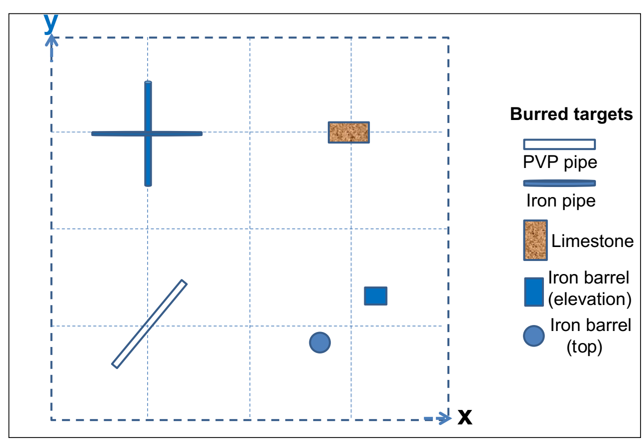

Fig. 11 The field experimental site was built up 20×20m, where five different targets were buried at the depths of 1–3 m. The five targets include PVP pipes, iron pipes, limestone, iron bar, and block, which have different sizes and physical properties

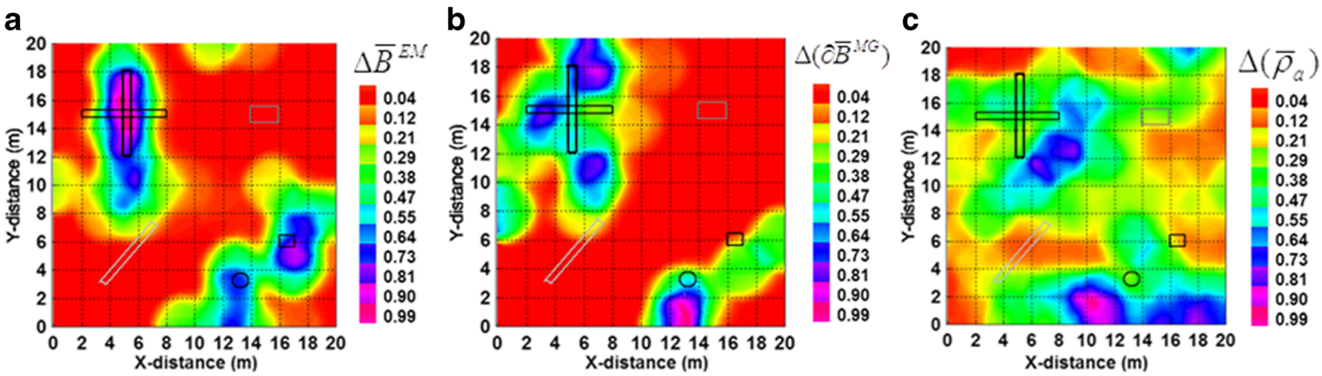

Fig. 12 Normalized anomaly images obtained from individually mapping with (a) EM-61, (b) magnetometer, and (c) OhmMapper

assembly of the metal detector comes first, the cesium vapor sensors of the magnetometer are place at 100 cm away from the center of the coils, and the dummy weight of the OhmMapper shall be place 60 cm away from the cesium vapor sensors. The 180-cm dipole cable connecting the tow cable of the OhmMapper to the optical wand inside the dummy weight was replaced by the 400-cm cable to facilitate the routing of the cable around the coil assembly without affecting the distance between the cesium vapor sensor and the dummy weight. Accordingly, in our first design, we took all above constrains and recommendations into considerations; the implemented design was quite long. The total length of the cart (Fig. 9) was 275 cm as shown below in Fig. 8. After manufacturing the first cart, we found that the size is quite unacceptable due to difficult movement of the cart in a real site. In order to reduce the size, we focused on the interference that may occur among the scanners when getting them close to each other. Many trials have been conducted in the field for checking the interference effects.

Initial assessments at the beginning of the project showed that putting the scanners next to each other resulted in producing huge interference. In fact, the scanners represented possible targets (anomalies) to each other. The first step we took to eliminate the interference was placing two scanners away from each other at a safe distance where no interference took place, powering them on, and then bringing them closer to each other till we reach the minimum distance where detected interference is considered negligible. This procedure was repeated with all the scanners and the minimum distance were recorded for cart design later on. The assessments and experiments showed that the magnetometer was the most sensitive among the three scanners. So, the second thing we did to eliminate the interference is isolating the magnetometer sensors using a metallic shield so that the sensors can only be altered with anomalies beneath them without being affected with nearby components and items. By comparing the measurement results of the integrated system with the data measured by the individual system, we may quantify the interference of the sub-systems. This step helped us minimize the size of the cart to the dimensions shown in Fig. 9 and finally reduced the length of the cart to be only 135 cm which is a 51% reduction. Figure 10 is taken during a real test conducted to make sure that all the systems were working properly without interference each other. In the final cart, the distance between the cesium sensors and the metal detector loop assembly has been completely removed, the space between the console shelves and the loop assembly has been reduced to 35cm, and the wooden bar used for hooking the OhmMapper sensors chain has been totally removed, and the sensor chain was hooked at the front side of the cart. The top shelf was reserved of the ECU, to which all systems will be connected.

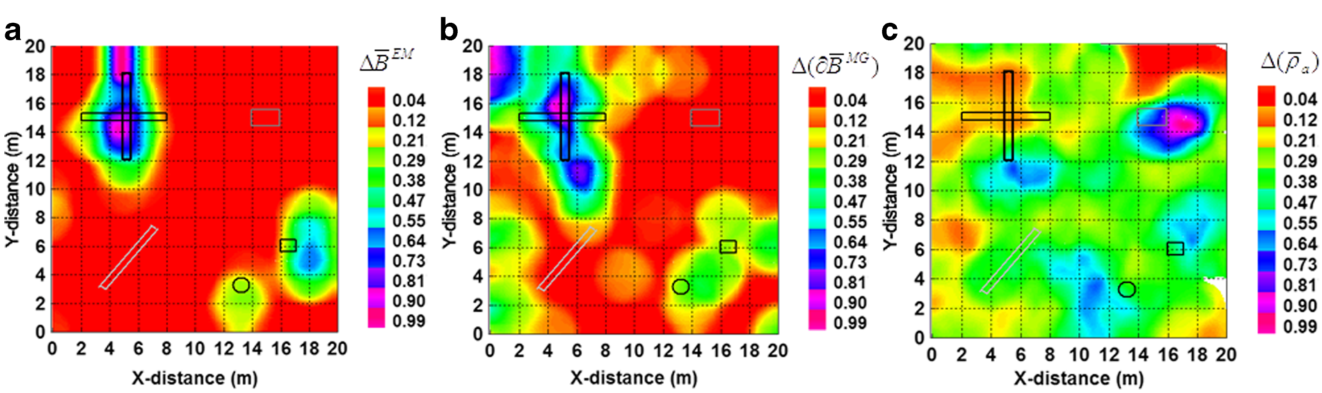

Fig. 13 Normalised anomaly images obtained from the new cluster system measuring (a) the secondary electromagnetic filed, (b) magnetic field, and (c) apparent resistivity

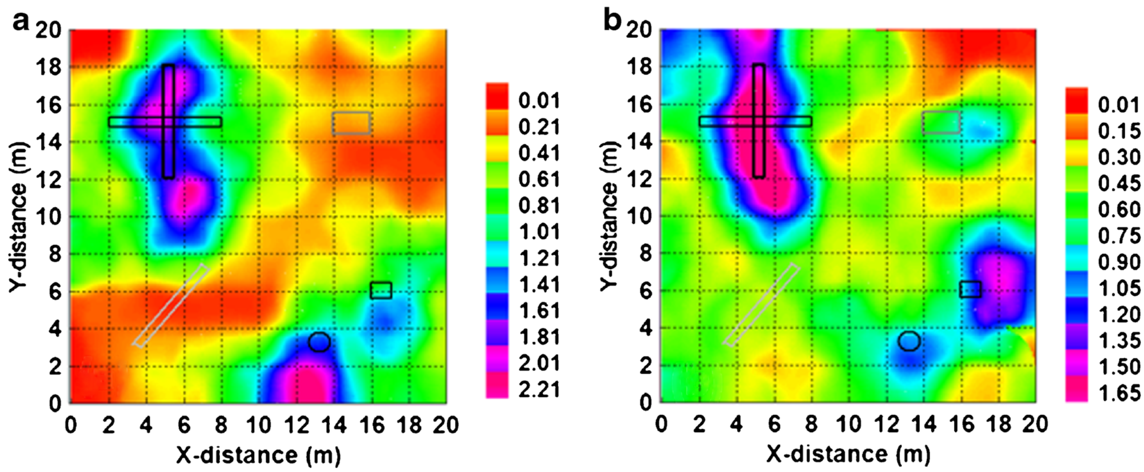

Fig. 14 Combined normalized anomaly (CAN) images obtained from mapping surveys using (a) three scanners and (b) the new cluster system

Field experiments

In order to test the new system, we built up a 20 × 20-m experimental site (see Fig. 11) where five different targets were buried at the depths of 1–3 m. The five targets include PVP pipes (40cm depth, 30cm diameter, 6m length), iron pipes (70–90cm depth, 30cm diameter, 6m length), limestone (35cm depth, 2×1×1 m^3 size), iron bar (35–121cm depth, 56cm diameter), and iron block (35cm depth, 91cm length, 56cm diameter), which have different sizes and physical properties. The soil profile of the site was found as follows: horizon A (0–80cm), made of fresh fully decomposed organic matter and well mixed with less minerals, color of dark brown; and horizon B (80–180cm). Two independent surveys were separately carried out along 11 lines parallel to the x-axis with a 2-m space. The first survey individually uses three scanners and produces three anomaly images. The second survey employs the new system and also yields three anomaly images, which are integrated into a single anomaly image. The approximate time taken by each individual scanner varied from 45 to 60 min. The longest time was taken by the OhmMapper since it requires realignment of the sensors for each line we scanned. So, the total time to scan the test field with three devices individually is 150 min. Scanning the same test field with the new system (all scanners on the same cart) took around 60 min. So, the result was saving 60% of the time. The data processing of the new system involves the following calculations:

(a) Normalized EM-61 anomaly

$$\Delta \overline{B}_i^{EM} = \frac{1}{3}\sum_{j=1}^{3}\frac{\left|B_i^{(j)}-B_i^{(4)}\right|}{\max\limits_i\left\{\left|B_i^{(j)}-B_i^{(4)}\right|\right\}}, \quad (i=1,2,\ldots,N) \tag{1}$$

(b) Normalized magnetometer anomaly

$$\Delta\left(\partial \overline{B}_i^{MG}\right) = \frac{1}{2}\left\{\frac{\left|\partial_x\left(B_i-B_i^0\right)\right|}{\max\limits_i\left|\partial_x\left(B_i-B_i^0\right)\right|}+\frac{\left|\partial_{xx}\left(B_i-B_i^0\right)\right|}{\max\limits_i\left|\partial_{xx}\left(B_i-B_i^0\right)\right|}\right\}, \quad (i=1,2,,,,,N) \tag{2}$$

(c) Normalized OhmMapper anomaly

$$\Delta\left(\overline{\rho}_a\right)_i = \frac{\left|(\rho_a)_i-(\rho_a^0)_i\right|}{\max\limits_i\left\{\left|(\rho_a)_i-(\rho_a^0)_i\right|\right\}}, \quad (i=1,2,\ldots,N) \tag{3}$$

(d) Combined normalized anomaly (CNA)

$$CNA = \left[\Delta \overline{B}_i^{EM} + \Delta\left(\partial \overline{B}_i^{MG}\right) + \Delta\left(\overline{\rho}_a\right)_i\right], \quad (i=1,2,\ldots,N) \tag{4}$$

Here, the subscript "i" and superscript "0" stand for the observation position (x_i, y_i) and the background value, respectively. The background values can be obtained from the trend analysis. The integer N is the total number of the observation positions. Basing on the formulae, we wrote a computer program that processes the three types of the date and produces the CNA image in a couple of minutes with a single execution of the computer code.

Figure 12 shows the results obtained from the individually mapping with scanner EM-61, magnetometer, and OhmMapper, respectively. From these results, one can see that the iron pipes, iron bar, and iron block are clearly indicated with strong anomaly values by both EM-61 and magnetometer scanners, but the images fail in mapping the limestone block and PVP pipes because of low conductivities, while OhmMapper picked up the anomaly of the limestone but missed out the PVP pipe. In principle, the resistivity measurement (OhmMapper) should be able to find the PVP pipes because of zero conductivity, but in this case, the electrode space (2.5m) may be relatively much larger than the radius of the PVP pipe so that its anomaly becomes too weak.

Figure 13 shows the three anomaly images obtained from the cluster system. Comparing these results with images given in Fig. 12, one may find that they are very similar. Adding the three anomaly images, we have the CNA images shown in Fig. 14 from the two independent surveys. The two images both have the apparent anomalous values over the buried targets. It is shown that our new integrated scanning system archives the capabilities of all three scanners mapping these buried targets but is much more efficient in data acquisition and data processing, because of its only needing one operator, saving much field-working time and a fast comprehensive data processing.

Conclusions

A new fusion of geophysical scanners is developed for mapping different buried targets at the near-surface. The new cluster system includes EM-61 metal detector, magnetometer, and OhmMapper scanners, all of which are controlled by an innovative electric central unit that makes the three-type data acquisitions become simultaneous and more efficient. A new computer program is also developed for the data processing and enables us to fast produce three normalized anomaly images and CNA image from the three kinds of observed data.

The test field is a 20 × 20-m square-shaped piece of land with known materials (anomalies) buried underneath the surface at known depth. The field experiments were conducted to measure the saving in time and operators. It is shown that the new system may save 60% of the field working time. In addition, each of the individual scanners has its own operator, except for the OhmMapper which needs two operators. The total number of operators is four while the new system needs only two. This also resulted in lowering the number of operators by half. It is concluded that the new cluster of the scanners becomes an effective and efficient integrated mapping tool for detecting the near-surface targets.

Future developments are taken into considerations. Some of those developments may be involved: (1) adding another scanner, e.g., ground-penetrating radar, (2) the electronic controller to include extra features, like build-in GPS, integrated distance meter, and advanced interface to be able to check results on site.

Acknowledgements The authors would like to thank KACST for supporting this work and acknowledge the great help and support from who participated in works carried out for this study.

Declarations

Conflict of interest The authors declare that they have no competing interests.

References

Breiner S (1999) Applications manual for portable Agnetometers (Geometrics Inc)
Geometrics (1995) G-858 MagMapper operation manual. Geometrics Inc., Sunnydale
Geometrics (2001) DataMap OhmMapper User Guide, 29006-01, Rev 3.0, Manual 9007-01 Rev. A (Geometrics Inc.)
Geonics (2010) EM61-MK2A, Time domain metal detector (Geonics Limited)
Hinze W, Von Frese R, Saad A (2013) Magnetic data acquisition. In: Gravity and Magnetic exploration: principles, practices, and applications. Cambridge University Press, Cambridge, pp 276–299
Keating P, Sailhac P (2004) Use of the analytic signal to identify magnetic anomalies due to kimberlite pipes. Geophy 69:180–190
Loke MH (2011) Electrical resistivity surveys and data interpretation. in Gupta, H (ed.), Solid Earth Geophysics Encyclopaedia (2nd Edition) "Electrical & Electromagnetic" Springer-Verlag, 276-283
Telford WM, Geldart LP, Sheriff RE (1990) Applied Geophysics, second edition (Cambridge University Press)
Zhdanov MS (2017) Foundations of geophysical electromagnetic theory and methods, Elsevier, 770 pp.